Invest Clin 66(3): 269 - 281, 2025 https://doi.org/10.54817/IC.v66n3a04

Experimental study on the regulatory effect of Qinggan Dongyin on T lymphocyte homeostasis in MRL/lpr mice.

Nan Jiang[1#], Xiangqing Che[1#], Haiyan Han[2], Haoyang Xin[1], Shuo Wang[2], Jingpeng Li[1] and Shuo Zhang[3]

[1]Department of Rheumatology and Immunology, Second Affiliated Hospital of Tianjin University of TCM, Tianjin, China.
[2]Tianjin University of Traditional Chinese Medicine, Tianjin, China.
[3]Department of Pneumonology, Second Affiliated Hospital of Tianjin University of TCM, Tianjin, China.
[#]These authors contributed equally to this work and share first authorship.

Keywords: lupus erythematosus, systemic, Qinggan Dongyin, T-lymphocytes, signal pathways, cGAS-STING protein, mouse.

Abstract. Systemic lupus erythematosus (SLE) is an autoimmune disease marked by autoantibody overproduction and increased infection risk, even with current treatments. Dysregulated T lymphocyte homeostasis contributes to SLE progression, prompting exploration of immunomodulatory therapies. This study evaluated the effects of Qinggan Dongyin (QGDY), a compound of traditional Chinese medicine, in a murine SLE model. Twelve female MRL/lpr mice were randomly divided into model and QGDY treatment groups (n=6 each), with age-matched C57BL/6 mice as controls. QGDY (5 mL/kg/day) was administered via gavage for two weeks; controls received saline. Flow cytometry analyzed T cell subsets (CD4+, CD8+, Treg, Th1, Th2, Th17), ELISA measured plasma cytokines (IFN-γ, IL-6, TNF-α, IL-17A, TGF-β), HE staining assessed lung and kidney pathology, and qPCR evaluated cGAS and STING expression. Compared to the model group, QGDY significantly restored T cell balance by increasing CD4+, CD8+, and Treg cells and reducing Th1, Th2, and Th17 cells ($p<0.01$). QGDY also lowered pro-inflammatory cytokine levels ($p<0.05$), improved organ histopathology, and normalized elevated cGAS and STING expression ($p<0.01$). These findings indicate that QGDY exerts immunomodulatory effects in SLE, suggesting therapeutic potential through the regulation of T cell function and inflammatory signalling pathways.

Corresponding author: Shuo Zhang. Department of Pneumonology, Second Affiliated Hospital of Tianjin University of TCM. No. 69, Zengchan Street, Hebei District, Tianjin 300250, China. Tel: +86 13821172351. Email: zhangshuottt@126.com

Estudio experimental sobre el efecto regulador de Qinggan Dongyin en la homeostasis de los linfocitos T en ratones MRL/lpr.

Invest Clin 2025; 66 (3): 269 – 281

Palabras clave: lupus eritematoso sistémico; Qinggan Dongyin linfocitos T; vías de señalización; proteínas cGAS y STING de ratón.

Resumen. El lupus eritematoso sistémico (LES) es una enfermedad autoinmune caracterizada por la sobreproducción de autoanticuerpos y un aumento del riesgo de infección, incluso con los tratamientos actuales. La homeostasis desrregulada de los linfocitos T contribuye a la progresión del LES, lo que impulsa la exploración de terapias inmunomoduladoras. Este estudio evaluó los efectos de Qinggan Dongyin (QGDY), un medicamento tradicional chino compuesto, en un modelo murino de LES. Doce ratones hembras MRL/lpr fueron divididas aleatoriamente un grupo modelo y un grupo de tratamiento con QGDY (n=6 en cada grupo), con ratones C57BL/6 emparejados por edad como controles. Se administró QGDY (5 mL/kg/día) por medio de sonda durante dos semanas; los controles recibieron solución salina. Se analizó la subpoblación de células T (CD4+, CD8+, Treg, Th1, Th2, Th17) mediante citometría de flujo, se midieron las citoquinas plasmáticas (IFN-γ, IL-6, TNF-α, IL-17A, TGF-β) por ELISA, se evaluó la patología pulmonar y renal mediante tinción con HE, y se evaluó la expresión de cGAS y STING mediante qPCR. En comparación con el grupo modelo, QGDY restauró significativamente el equilibrio de las células T al aumentar las células CD4+, CD8+ y Treg y reducir las células Th1, Th2 y Th17 ($p<0,01$). QGDY también disminuyó los niveles de citoquinas proinflamatorias ($p<0,05$), mejoró la histopatología de órganos y normalizó la expresión elevada de cGAS y STING ($p<0,01$). Estos hallazgos indican que QGDY ejerce efectos inmunomoduladores en el LES, sugiriendo un potencial terapéutico a través de la regulación de la función de las células T y las vías de señalización inflamatoria.

Received: 25-03-2025 Accepted: 24-06-2025

INTRODUCTION

Systemic lupus erythematosus (SLE) is a chronic autoimmune disorder marked by the overproduction of autoantibodies and the formation of immune complexes, which can impact various organs and systems [1]. While advancements in diagnosis and treatment have enhanced the survival rate of SLE patients, the mortality rate remains high [2]. Infections, particularly in the context of the recent global spread of SARS-CoV-2, have emerged as a significant cause of death among SLE patients [3]. Research indicates that SLE patients face significantly higher risks compared to the general population [4-5].

In autoimmune diseases such as SLE, infection and autoimmune response interact with each other. On the one hand, infection can destroy the immune tolerance to autoantigens and induce the development of autoimmune diseases in individuals with a genetic predisposition. The persistent infection of pathogens may lead to the aggrava-

tion of disease activity via molecular simulation, bystander activation, epitope diffusion or polyclonal activation [6]. On the other hand, high disease activity, immune dysregulation, and drugs (such as glucocorticoids and immunosuppressants) induce immune deficiency and organ failure [2].

Lymphocytes are key players in the pathogenesis of SLE [7,8]. Dysregulation of T lymphocytes, including changes in cell count, subset distribution, and function, is implicated in the progression of SLE and is closely linked to infection risk [9]. Specifically, a reduction in CD4+ T cells is the most frequently reported hematological abnormality in SLE, often correlating with a higher risk of infection [10]. Meanwhile, CD8+ T cells, which are cytotoxic and typically destroy target cells through the release of perforin and granzyme, show impaired function in SLE patients. This dysfunction leads to increased risks of both infections and autoimmune reactions [11]. In addition, Treg, Th1, Th2, and Th17 cells are important subsets of CD4+ T lymphocytes, and their distribution and function are significantly disordered. The absolute decrease in the number of Tregs is associated with immune tolerance disruption and the subsequent worsened disease activity and increased infection risk in SLE patients [12]. Meanwhile, the increase in Th cell activity may enhance the local tissue inflammation and damage important target organs such as the kidneys [13-15]. Therefore, regulation of the T lymphocyte homeostasis in SLE patients may effectively control the autoimmune response while maintaining immune function and preventing infection, hopefully providing an effective treatment method to meet the urgent clinical need.

Qinggan Dongyin (QGDY) is a compound preparation consisting of multiple Chinese herbal medicines, it was developed based on the experience of Academician Zhang Boli's team in the prevention and control of a novel coronavirus infection in Wuhan [16], and the main therapeutic goal of this prescription is to protect vital qi (defined as enhancing the body's defenses and promoting recovery in traditional Chinese medicine), resist exopathogens, and clear away heat and toxic material. Clinical studies have shown that QGDY is highly effective in preventing respiratory tract infections with a favorable safety profile [16]. Network pharmacological studies have shown that QGDY plays a regulatory role in various viral infections by regulating the immune-inflammatory response caused by infection[17]. Pharmacological studies have also found that QGDY has antioxidant and anti-inflammatory activities, and significantly regulates the number of lymphocytes, the level of interleukin and the release of TNF-α in in peripheral blood [18-19]. The usefulness of QGDY in infections has been reported, but the experience with this substance in autoimmune diseases has not. In the present study, the SLE mouse model (MRL/lpr mouse) was intervened with QGDY. The distribution of T lymphocyte subsets, expression of related cytokines, and pathological damage of lung and kidney in these mice were observed to clarify the regulatory effects of QGDY on T lymphocyte homeostasis and immune response in MRL/lpr mice, providing supportive data for adjuvant treatment of SLE and risk reduction of infection.

MATERIALS AND METHODS

Instruments and reagents

Main instruments included BD FACSCalibur flow cytometer (BD, USA), ELX800 microplate reader (BioTek, USA), inverted microscope (Nikon TS2), desktop high-speed refrigerated microcentrifuge (D3024R, DLAB Scientific Co., Ltd), and fluorescence quantitative PCR instrument (Stepone plus, ABI, USA).

Main reagents included FITC anti-mouse CD3 antibody (item number: E-AB-F1013C), PE anti-mouse CD4 antibody (item number: E-AB-F1097D), PerCP anti-mouse CD8a antibody item number: E-AB-F1104F), APC anti-mouse Foxp3 antibody (item

number: E-AB-F1238E), APC anti-mouse CD183/CXCR3 antibody (item number: E-AB-F1114E), APC anti-human/mouse CD44 antibody (item number: E-AB-F1100E), APC anti-mouse IL-17A antibody (item number: E-AB-F1272E), all antibodies were purchased from Elabscience. Other reagents were hematoxylin (Servicebio, item number: G1004-100ML), eosin staining solution (Solarbio, item number: G1108), mouse interferon gamma (IFN-γ) ELISA kit (Meimian, item number: MM-0182M2), mouse IL-6 ELISA kit (Meimian, item number: MM-0163M2), mouse TNF-α ELISA kit (Meimian, item number: MM-0180R2), mouse IL-17A ELISA kit (Meimian, item number: MM-0180R2), mouse TGF-β ELISA kit (Meimian, item number: MM-0689M2), mouse PFP ELISA kit (Meimian, item number: MM-4504M2), Trizol reagent (Vazyme, item number: R401-1), and MonAmp™ SYBR® Green qPCR Mix (Wuhan Monad Biotechnology Co., Ltd., item number: MQ10201S).

Experimental animals and grouping

Twelve female MRL/lpr mice, aged eight weeks, were randomly assigned to two groups: the model group and the QGDY group, with six mice in each. Additionally, six age-matched female C57BL/6 mice were used as the control group. All mice were purchased from SPF (Beijing) Biotechnology Co. Ltd. The mice were housed in a room with natural lighting, maintained at a temperature of 20-24°C, with proper ventilation and humidity control. After a 1-week acclimatization period with free access to food and water, the experiment commenced once the mice were in optimal health. The study was approved by the Animal Ethics Committee (Approval No. IRM/IRM/2-IACUC-2403-126).

Preparation and concentration of QGDY

QGDY consisted of *Astragalus membranaceus* 18g, *Polygonum cuspidatum* 18g, stir-baked *Fructus arctii* 18g, *Belamcanda sinensis* 12g, *Platycodon grandiflorum* 12g, *Radix paeoniae rubra* 12g, *Perilla frutescens* leaves 12g, honeysuckle 18g, charred hawthorn 12g, and licorice 6g. The dosage was calculated based on the "Table of equivalent dose ratios between humans and animals by body surface area" [1]. 0.3588g, i.e., 17.94g/kg, of QGDY crude drug, was required for a 20g mouse per day, assuming that the coefficient between humans (70kg) and mice (20g) was 0.0026 and that 138g of the crude drug was needed for each patient daily. All medicinal herbs were boiled twice, and the decoction was combined, filtered, and concentrated to obtain a medicinal solution containing 3.6g/mL of crude drug. Animals in the QGDY group were given QGDY by gavage at a dose of 5mL/kg, while those in the control group and the model group were given normal saline by gavage at a dose of 5ml/kg for two consecutive weeks, once a day. Gavage was administered at a fixed time (9:00-10:00 am) every day without fasting.

Sample collection and processing

After two weeks of intragastric administration, mice in each group were anesthetized with 1% pentobarbital sodium to reduce their stress response. Plasma was collected, and the mice were then sacrificed to collect corresponding samples. (1) Plasma was collected. Briefly, the blood was collected from the eyeballs of mice, and placed in a centrifuge tube containing EDTA for anticoagulation at RT for two hours, followed by centrifugation at 3500rpm for 15 minutes. The supernatant was collected and frozen at −80℃ in an EP tube for ELISA. (2) Following euthanasia, the abdominal cavity was opened to remove the lungs. The left lung was fixed in 4% paraformaldehyde for histopathological analysis, while the right lung was collected for PCR testing. (3) After sacrificing the mice with various treatments, the abdominal cavity was opened to extract the left kidney, which was fixed in 4% paraformaldehyde for pathological examination. In contrast, the right kidney was stored at −80℃ for potential future analysis or as a

backup sample. Additionally, the spleen was removed and placed in PBS for subsequent flow cytometry analysis.

Testing indexes and methods

Flow cytometry

Splenic tissue was sliced, ground and filtered, and the tissue filtrate was used to isolate monocytes. Briefly, an appropriate amount of separation solution of Lymphoprep (AN1001967) from Shanghai Shanjin Biotechnology Co., Ltd (Shanghai, China) was added to the centrifuge tube, and the diluted tissue filtrate was placed on top of the separation solution, with attention to keep the interface clear between the two liquid layers. The tube was centrifuged using a horizontal rotor at 500 x g for 20 minutes at RT. After centrifugation, layers were seen: the top layer contained the diluted plasma, the middle layer was the transparent separation solution, with a white membrane layer between the plasma and the separation solution, which was the lymphocyte layer, and the red blood cells and granulocytes gathered at the bottom of the centrifugation tube. Cells in the white membrane were carefully removed and placed in a clean 15mL centrifuge tube, and washed with 10 mL PBS, followed by centrifugation at 250×g for 10 minutes. The supernatant was discarded, 5mL PBS was added to resuspend the cells, and the cells were centrifuged at 250 × g for 10 minutes. This step was repeated twice. After centrifugation, the supernatant was discarded, and the cells were resuspended. 1×10^5 cells and 100μL (1 ×) Binding Buffer were added to each sample tube, and staining was performed. Cells were first washed twice with PBS. Subsequently, Cyto-Fast Fix/Perm Buffer was added to fix the cells, which were then incubated at 4℃ for 20 minutes before being rewashed with PBS. APC-conjugated anti-mouse Foxp3 antibody (ab215206) for Treg cells, CD4 antibody (ab237722) for CD4+ T cells, CD8 antibody (ab237709) for CD8+ T, IFN-γ antibody (ab280353) for Th1 cells, IL-4 antibody (ab225638) for Th2 cells, and IL-17A antibody (ab302922) for Th17 cells from Abcam biotechnology company (UK) was added and incubated for 15 minutes. An additional 400 μL of 1x Binding Buffer was added to each tube, followed by filtration of the mixture. A total of 10,000 cells were collected from the stained samples using a BD FACSCalibur flow cytometer.

ELISA

Plasma levels of IFN-γ (H025-1-2), IL-17A (H014-2), TGF-β (H034-1-1) were purchased from the Nanjing Jiancheng Bioengineering Institute (Nanjing, China), and the IL-6 (ab222503, Abcam), TNF-α (ab183218, Abcam), and perforin protein (PFP) (ab114201, Abcam) were obtained from Abcam biotechnology company for inflammatory factor detection using ELISA kits following the manufacturer's protocols. The OD of each well was detected with an ELX800 microplate reader at a wavelength of 450 nm.

HE staining

Lung and kidney tissues fixed in 4% paraformaldehyde underwent dehydration, clarification, paraffin embedding, and sectioning. Following HE staining, the pathological changes in the lungs and kidneys were examined for each group (control group, model group, and QGDY group), under a light microscope at magnifications of 200x (top row) and 400x (bottom row). For the histological parameters, the inflammatory cell infiltration (neutrophils and lymphocytes), alveolar structure changes (Alveolar wall thickness, alveolar cavity, and interstitial fibrosis) were examined in lung tissues, while the vacuoles, glomerular consolidation, glomerular structure change, inflammatory cell infiltration, and cell proliferation were examined in kidney tissues.

Quantitative PCR (qPCR)

Total RNAs were extracted. Briefly, tissues, adherent cells, and whole blood sam-

ples were pretreated and lysed using an RNA extraction solution, followed by centrifugation and precipitation of RNA. The concentration and purity of RNAs were determined. Next, reverse transcription was performed. A reverse transcription reaction system containing a gDNA digestion mixture and Hifair® III SuperMix was prepared, and the reaction program was set (25℃, 55℃, and 85℃). The quantitative PCR was conducted. A PCR reaction system was prepared using MonAmp™ SYBR® Green qPCR Mix and primers, and temperature cycles, including pre-denaturation, denaturation, annealing, elongation, and melting curves, were set. Finally, the fold expressions of the target genes were calculated using the 2^-ΔΔCt method to evaluate their relative expression levels.

The sequences of primers used included: Primers for inflammation-related genes of cyclic GMP-AMP synthase (cGAS): forward (cGAS-F): TATGGCGGTGACACACTTCC, and reverse (cGAS-R): GTCAGGACAGGTGAGCAGAC; primers for mouse stimulator of interferon gene (STING): forward (STING-F): TGTCTGGCTGAAGAGCTGTG, and reverse (STING-R): CGATTCTTGATGCCAGCACG.

Statistical analysis

Statistical analysis was performed using the IBM SPSS Statistics 26 software. Quantitative data were expressed as mean±standard deviation, while measurement data were reported as median (interquartile range) [M (IQR)]. For comparisons between groups, normally distributed data were analyzed using one-way ANOVA followed by Tukey's test, whereas non-normally distributed data were evaluated using the non-parametric Kruskal-Wallis test, $p<0.05$ was considered statistically significant.

RESULTS

Distribution of immune cells and Treg lymphocytes in the spleens of mice in each group

Significant differences were observed in the expression levels of various lymphocyte subsets between the groups. The model group exhibited a notable decrease in CD4+ T, CD8+ T, and Treg cells, while Th1, Th2, and Th17 lymphocytes were elevated ($p<0.01$). In contrast, the QGDY group showed a reversal of these trends, with increased levels of CD4+ T, CD8+ T, and Treg cells and decreased levels of Th1, Th2, and Th17 lymphocytes ($p<0.01$) (Table 1).

Concentrations of plasma IFN-γ, IL-6, TNF-α, IL-17A, TGF-β and PFP in each group of mice

Significant changes in plasma cytokine levels were observed between the groups. The

Table 1. Distribution of CD4 + T, CD8 + T, Th1, Th2, Th17 and Treg cells in the spleen of mice in each group.

	Control group (n=6)	Model group (n=6)	QGDY group (n=6)
CD4+ T (%)	19.60 ± 1.05	15.40 ± 0.30***	17.60 ± 0.57###
CD8+ T (%)	12.65 ± 1.10	6.33 ± 0.46***	9.52 ± 0.19###
Th1 (%)	0.85 ± 0.26	3.40 ± 0.51**	1.60 ± 0.11##
Th2 (%)	0.76 ± 0.12	3.26 ± 0.71***	1.58 ± 0.05###
Th17 (%)	1.34 ± 0.34	2.86 ± 0.16***	1.95 ± 0.15###
Treg (%)	2.59 ± 0.14	0.59 ± 0.26**	1.61 ± 0.08##

Note: Cells of CD4-positive T cells (CD4+ T), CD8-positive T cells (CD8+ T), T-helper 1 cells (Th1), T-helper 2 cells (Th2), T-helper 17 cells (Th17), Regulatory T cells (Treg) in model and treatment group compared with the control group using one-way ANOVA method, and the mean ± standard deviation (SD) is used for the result representation. **p<0.01, ***p<0.001; compared with the model group, ###p<0.001, ##p<0.01.

model group exhibited higher levels of IFN-γ, IL-6, TNF-α, IL-17A, and TGF-β ($p<0.05$), while the level of PFP was lower ($p<0.05$). In the QGDY group, the levels of IFN-γ, TNF-α, IL-17A, and TGF-β were reduced compared to the model group ($p<0.05$) (Table 2).

Pathological analysis of lung and kidney tissues in each group of mice

In the control group, the pulmonary alveoli were evenly distributed with neatly arranged cells, the alveolar wall was thin and uniform, and the alveolar cavity was clear and visible. In contrast, the model group exhibited disordered cell arrangement, thickened alveolar walls and narrowing or even occlusion of the alveolar cavities, increased lung parenchyma, and more severe inflammation. The QGDY group showed improved cell arrangement, reduced lung parenchyma, and less inflammation compared to the model group (Fig. 1).

Table 2. Concentrations of IFN-γ, IL-6, TNF-α, IL-17A, TGF-β and PFP in the plasma of mice in each group.

	Control group (n=6)	Model group (n=6)	QGDY group (n=6)
IFN-γ (ng/L)	120.56 ± 42.44	461.76 ± 304.88*	168.99 ± 36.32#
IL-6 (pg/mL)	31.05 ± 11.39	86.16 ± 71.44*	28.28 ± 45.16
TNF-α (ng/L)	80.94 ± 46.70	385.03 ± 238.84**	189.11 ± 204.82#
IL-17A (pg/mL)	20.26 ± 6.09	105.87 ± 46.26**	45.99 ± 42.64#
TGF-β (ng/L)	24.53 ± 24.68	190.48 ± 148.21**	62.24 ± 40.51#
PFP (ng/L)	49.83 ± 24.07	11.34 ± 7.53**	31.21 ± 17.88

Note: The cytokines of Interferon-gamma (IFN-γ), Interleukin-6 (IL-6), Tumor Necrosis Factor-α (TNF-α), Interleukin-17A (IL-17A), Transforming Growth Factor-beta (TGF-β), Perforin (PFP) in model and treatment groups compared with the control group using One-way ANOVA method, and the mean ± standard deviation (SD) is used for the result representation. *$p<0.05$, **$p<0.01$; compared with the model group, #$p<0.05$.

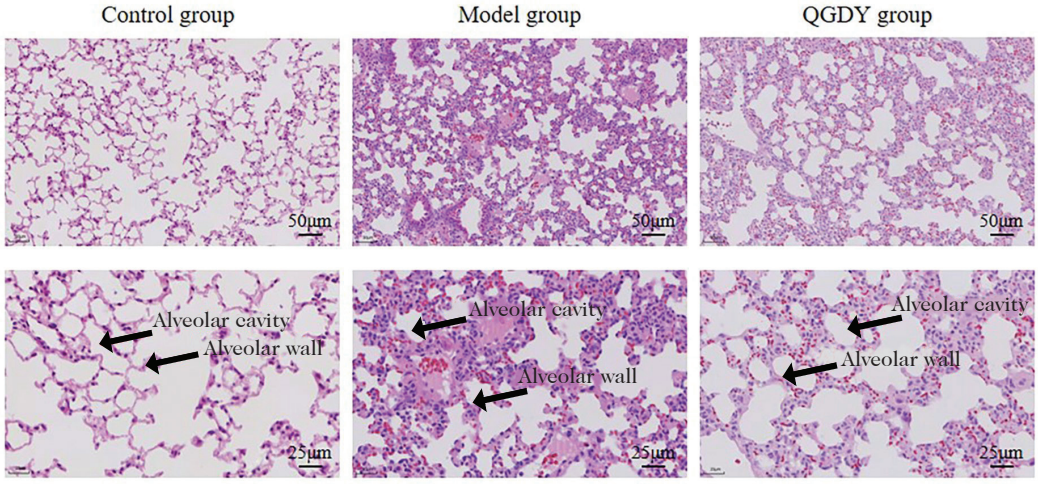

Fig. 1. Histopathological changes in lung tissues of different groups (HE staining).

Inflammation was defined as the presence of increased numbers of inflammatory cells (primarily neutrophils and mononuclear cells) within the alveolar spaces and interstitial areas.

Overall, the degree of inflammation was assessed by evaluating the density and distribution of these cells. The control group showed minimal to no inflammation, while the model group exhibited significant infiltration of inflammatory cells. The QGDY group showed a reduction in inflammatory cell infiltration compared to the model group.

Regarding kidney pathology, the control group had intact glomerular morphology with minimal inflammatory cell infiltration. The model group displayed glomerular consolidation, vacuoles, proliferation, and significant inflammatory cell infiltration. The QGDY group had more orderly glomerular structures and reduced inflammation compared to the model group (Fig. 2).

Expression of cGAS and STING

Expression levels of cGAS and STING varied significantly among the control, model, and QGDY groups ($p<0.01$). In the model group, elevated cGAS and STING expressions were noted compared to the control group, reflecting heightened immune activation. Conversely, the QGDY group exhibited reduced cGAS and STING levels, nearing those of the control group, implying that QGDY might modulate this critical immune signalling pathway (Fig. 3).

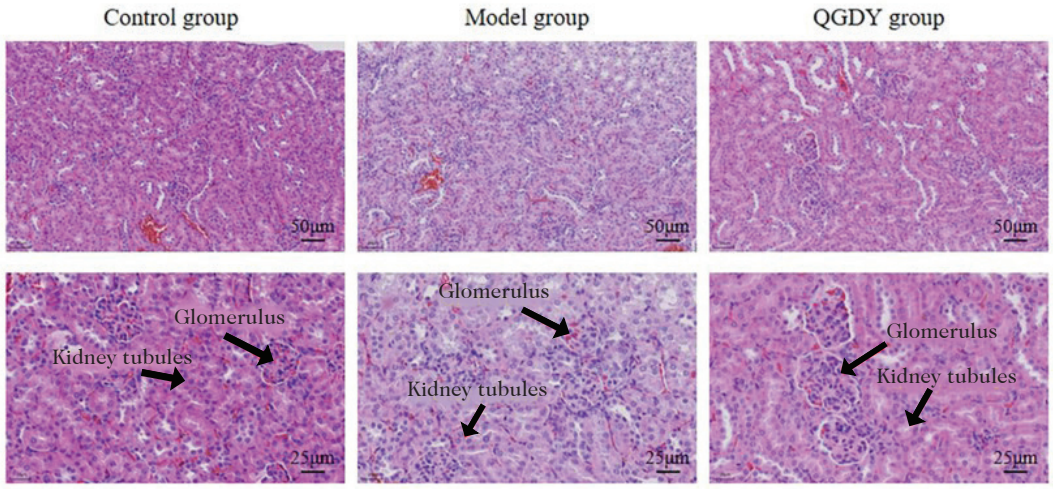

Fig. 2. Pathological analysis of kidney tissue in each group of mice.

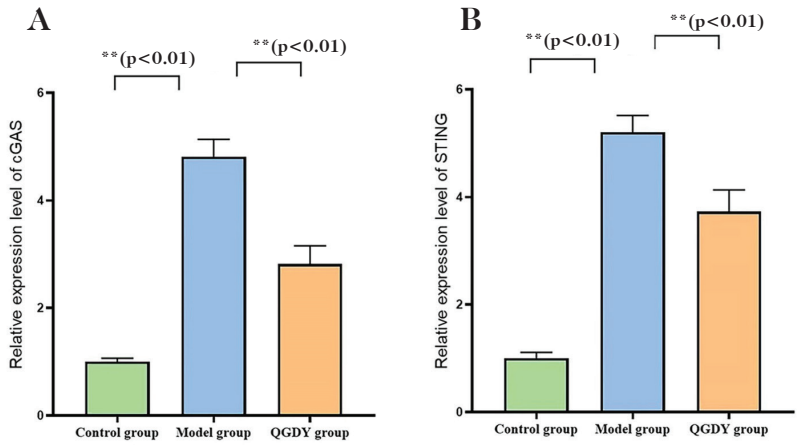

Fig. 3. qPCR for the expression of cyclic GMP-AMP synthase (cGAS) and stimulator of interferon gene (STING). (A) The relative expression level of cGAS, and (B) the relative expression level of STING.

DISCUSSION

The regulatory effect of QGDY on T lymphocyte homeostasis and related immune signalling pathways in MRL/lpr mouse models was investigated in the present study. These model animals have characteristics similar to human SLE due to spontaneous mutations in the *lpr* gene (lymphoproliferation gene), including lymphocyte abnormalities, lymph node enlargement, excessive autoantibodies and glomerulonephritis [20], making it a classic model for studies on the immunopathological mechanism of SLE. The abnormal distribution and dysfunction of T lymphocyte subsets are one of the key factors in the pathogenesis of SLE[21]. Previous studies have revealed significant changes in the number of T subsets in MRL/lpr mice [22]. It was found in the present study that QGDY significantly improved the distribution of T lymphocytes in MRL/lpr mouse models, enhanced the expression of CD4+, CD8+ and Treg cells, and reduced the number of Th1, Th2 and Th17 cells. This prescription also effectively inhibited the levels of plasma inflammatory factors IFN-γ, IL-6, TNF-α, IL-17A and TGF-β, indicating its anti-inflammatory effect. The pathological evaluation showed that QGDY reduced the inflammation and damage to the lung and kidney and maintained the integrity of tissue structure. In addition, QGDY alleviated immune activation by regulating the cGAS and STING signalling pathways.

The findings offer fresh evidence supporting the potential use of QGDY in treating SLE. This study investigated the impact of QGDY on T cell function in MRL/lpr mice to elucidate its possible protective role in SLE. Dysfunctional T cells can elevate infection risk, particularly during immunosuppressive treatment. In SLE patients, compromised CD4+ T cell function not only affects autoantibody production but also weakens infection defense. Moreover, impaired CD8+ T cell function further exacerbates the infection risk [23]. Regulating T cell function is crucial for enhancing the autoimmune response and preventing infections in SLE. Our study demonstrated that QGDY significantly boosted the expression of CD4+ and CD8+ T cells, thereby strengthening the immune response to infections and lowering infection risk.

Additionally, QGDY reduced the number of Th1, Th2, and Th17 cells while increasing Treg cell expression. These changes are significant because Th1 and Th17 cells are often overactivated in SLE patients, driving inflammation through IFN-γ and IL-17 secretion and leading to tissue damage [24]. Thus, QGD's anti-inflammatory effects may mitigate SLE pathology by modulating the activity of these cells. Moreover, the cGAS-STING signalling pathway's role is noteworthy. QGDY significantly downregulated cGAS and STING expression, suggesting it curbs inflammation by inhibiting this pathway's overactivation. This mechanism likely impacts T lymphocyte differentiation and function, improving SLE's pathological state. Since the cGAS-STING pathway is linked to IFN-I production [25], the observed a reduction in related cytokines after QGDY intervention further supports its immune-regulating potential.

The high expression levels of TNF-α and IFN-γ are associated with the activation of Th1 lymphocytes and tissue damage [26]. The levels of plasma IFN-γ and TNF-α significantly decreased after treatment with QGDY, indicating the ability of this prescription to inhibit the activation of Th1 cells and alleviate the inflammation in involved organs. The increase of IL-6 and IL-17 is associated with Th17-mediated inflammatory response [27]. The changes in TGF-β expression may affect the function and quantity of Tregs and consequently, the immune tolerance. It was found in the present study that QGDY also significantly reduced the levels of these two cytokines, suggesting that it may reduce the inflammatory response via regulating the activity of Th17 cells. The changes in TGF-β level may affect the function and quantity of

Tregs [28], and the results of the present study showed that QGDY effectively enhanced the expression of Tregs, providing a basis for the improvement of immune tolerance. Pathological evaluation of the lungs and kidneys of mice demonstrated that QGDY significantly reduced tissue damage in MRL/lpr mice. The disordered cell arrangement and significant inflammation observed in the models were recovered to an improved cell structure and reduced inflammation after treatment with QGDY, indicating that QGDY can improve the pathological changes related to SLE by regulating T cell function and reducing inflammatory factors, providing new ideas for SLE treatment.

Modern studies have found that the components of QGDY are rich in various bioactive substances, including flavonoids, organic acids, and monoterpenes, which exert multiple regulatory effects on the human immune system. The medicinal herbs in QGDY, such as *Astragalus membranaceus* and honeysuckle, can enhance immunity and prevent inflammation [29], which are in line with the treatment goals of SLE. Progress has been made on the effects of individual medicinal herbs in QGDY on the function of T lymphocytes. For example, *Astragalus membranaceus* has been found to enhance the proliferation and differentiation of T lymphocytes and improve the immunity of body [29]. The active compounds contained in medicinal herbs such as *Polygonum cuspidatum* and stir-baked *Fructus arctii* regulate the cytokines produced by T lymphocytes and affect the function of these cells. Medicinal herbs such as *Belamcanda sinensis* and *Platycodon grandiflorum* have shown the potential to regulate the balance of T subsets, which can help improve the overactive state of the immune system. *Radix paeoniae rubra*, *Perilla frutescens* leaves, honeysuckle, charred hawthorn and Licorice are also involved in the regulation of T cell-mediated immune responses.

There are limitations in the present study. First, although the MRL/lpr mouse is a classical animal model, it cannot completely simulate the complex pathological process of human SLE, which may affect the clinical translation of the results. Second, the sample size was relatively small. In addition, the specific effects of individual components of QGDY on T cell subsets and the underlying mechanism(s) were not adequately explored, and an in-depth molecular investigation was not conducted. Also, the study focused mainly on short-term treatment effects and long-term safety and efficacy were not evaluated. Finally, clinically relevant indicators such as improvement in clinical symptoms, quality of life of patients, and biomarkers were not evaluated. These limitations reminded us that caution should be exercised in interpreting the findings and providing directions for improvement in subsequent studies. Future studies with samples from broad and diverse sources are needed for long-term efficacy evaluation and in-depth discussion of mechanisms further to verify the potential application of QGDY in clinical practice.

QGDY significantly improves T lymphocyte homeostasis, reduces the levels of inflammatory factors, and alleviates organ pathological damage in MRL/lpr mice. Meanwhile, this prescription effectively regulates the expression of immune-related signalling molecules such as cGAS and STING, making it a promising adjuvant therapy for SLE to reduce the risk of infection via regulating immune balance, and providing new ideas and data support for clinical treatment of SLE.

Ethics approval and consent to participate

This study was conducted following the principles of ethical animal research outlined in the Basel Declaration and the ethical guidelines by the International Council for Laboratory Animal Science (ICLAS). This study was conducted under the NC3Rs ARRIVE guidelines.

The experimental protocol was approved by the Institute of Radiation Medicine, Chinese Academy of Medical Sciences

and the Peking Union Medical College (Approval Number: IRM/2-IACUC-2403-126). Experimental animals underwent all procedures under anesthesia, and every effort was made to minimize their pain, suffering, and death.

Data availability statement

All data generated or analyzed during this study are included in this article.

Acknowledgements

Not applicable.

Funding

This work was supported by The Science & Technology Development Fund of Tianjin Education Commission for Higher Education (2023KJ166).

Conflict of interest

The authors declare that they have no conflict of interest.

ORCID numbers author

- Nan Jiang: 0009-0009-4753-4425;
- Xiangqing Che: 0009-0001-0207-1203
- Haiyan Han: 0009-0009-0386-9565
- Haoyang Xin: 0009-0009-9785-6764
- Shuo Wang: 0009-0000-5597-7757
- Jingpeng Li: 0009-0003-3136-6451
- Shuo Zhang: 0009-0005-6896-0029

Participation of each author

NJ and XC conceived of the study, HH, HX and SW participated in its design and coordination, JL and SZ helped to draft the manuscript. All authors read and approved the final manuscript.

REFERENCES

1. **Kiriakidou M, Ching CL**. Systemic Lupus Erythematosus. Ann Intern Med. 2020;172(11): ITC81-ITC96. *https://doi.org/10.7326/AITC202006020.*
2. **Singh BK, Singh S**. Systemic lupus erythematosus and infections. Reumatismo. 2020;72(3):154-169. *https://doi.org/10.4081/reumatismo.2020.1303.*
3. **Rao M, Mikdashi J.** A Framework to Overcome Challenges in the Management of Infections in Patients with Systemic Lupus Erythematosus. Open Access Rheumatol. 2023; 15:125-137. *https://doi.org/doi: 10.2147/OARRR.S295036.*
4. **Akhlaq A, Aamer S, Hasan KM, Muzammil TS, Sohail AH, Quazi MA, et al.** Systemic lupus erythematosus is associated with increased risk of mortality and acute kidney injury in patients with COVID-19 hospitalization: Insights from a National Inpatient Sample analysis. Lupus. 2024;33(3):248-254. *https://doi.org/10.1177/09612033241227027.*
5. **Solé C, Domingo S, Vidal X, Cortés-Hernández J**. Humoral and cellular response in convalescent COVID-19 lupus patients. Sci Rep. 2022;12(1):13787. *https://doi.org/10.1038/s41598-022-17334-5.*
6. **Rao AP, Patro D**. The Intricate Dance of Infections and Autoimmunity: An Interesting Paradox. Indian J Pediatr. 2024;91(9):941-948. *https://doi.org/10.1007/s12098-023-04928-8.*
7. **Kang N, Liu X, You X, Sun W, Haneef K, Sun X, Liu W**. Aberrant B-Cell Activation in Systemic Lupus Erythematosus. Kidney Dis (Basel). 2022;8(6):437-445. *https://doi.org/10.1159/000527213.*
8. **Li H, Boulougoura A, Endo Y, Tsokos GC**. Abnormalities of T cells in systemic lupus erythematosus: new insights in pathogenesis and therapeutic strategies. J Autoimmun. 2022; 132:102870. *https://doi.org/10.1016/j.jaut.2022.102870.*
9. **Ding M, Jin L, Zhao J, Yang L, Cui S, Wang X, et al.** Add-on sirolimus for the treatment of mild or moderate systemic lupus erythematosus via T lymphocyte sub-

sets balance. Lupus Sci Med. 2024;11(1): e001072. *https://doi.org/10.1136/lupus-2023-001072.*

10. **Zhang J, Zhang S, Qiao J, Qiu M, Li X**. Risk factors analysis and risk assessment model construction of systemic lupus erythematosus patients with infection. Lupus. 2023;32(1):119-128. *https://doi.org/10.1177/09612033221141255.*
11. **Chen PM, Tsokos GC**. The role of CD8+ T-cell systemic lupus erythematosus pathogenesis: an update. Curr Opin Rheumatol 2021;33(6):586-591. *https://doi.org/10.1097/BOR.0000000000000815.*
12. **Tsai YG, Liao PF, Hsiao KH, Wu HM, Lin CY, Yang KD**. Pathogenesis and novel therapeutics of regulatory T cell subsets and interleukin-2 therapy in systemic lupus erythematosus. Front Immunol 2023; 14:1230264. *https://doi.org/10.3389/fimmu.2023.1230264.*
13. **Talaat RM, Mohamed SF, Bassyouni IH, Raouf AA**. Th1/Th2/Th17/Treg cytokine imbalance in systemic lupus erythematosus (SLE) patients: Correlation with disease activity. Cytokine. 2015;72(2):146-53. *https://doi.org/10.1016/j.cyto.2014.12.027.*
14. **Dolff S, Bijl M, Huitema MG, Limburg PC, Kallenberg CG, Abdulahad WH**. Disturbed Th1, Th2, Th17 and T(reg) balance in patients with systemic lupus erythematosus. Clin Immunol. 2011;141(2):197-204. *https://doi.org/10.1016/j.clim.2011. 08.005.*
15. **Paquissi FC, Abensur H**. The Th17/IL-17 Axis and Kidney Diseases, With Focus on Lupus Nephritis. Front Med (Lausanne). 2021; 8:654912. *https://doi.org/10.3389/fmed.2021.654912.*
16. **Zan SJ, Wang K, Zhang S, Fu K, Zhou SY, Feng JH, et al.** A multicenter cohort study on "Qinggandong Decoction" for prevention of influenza. China J Tradit Chin Med Pharm 2023;38(5):1960-1966.
17. **Sun Y, Geng Q, Zhao Y, Li C, Chen SF**. Mechanism of action of Qinggandong decoction in the treatment of influenza based on network pharmacology and molecular docking. Hunan J Tradit Chin Med 2022; 38(01):144-152.
18. **Su R, Lu J, Xi ZN, Wang JB, Song XB, Zhang H, Miao L**. Qinggan Dongyin inhibits LPS-induced inflammation of RAW264.7 macrophages by regulating the NF-κB/iNOS/NO signaling pathway. J Tianjin Univ Tradit Chin Med. 2022;41(06):737-745.
19. **Ren M, Fu K, Zhou SY, Sun X**. Expert consensus on clinical application of "Qinggan Yin" series pharmaceutics. Tianjin J Tradi Chin Med. 2020;37(11):1201-1204.
20. **Yuan S, Zeng Y, Li J, Wang C, Li W, He Z, et al.** Phenotypical changes and clinical significance of CD4+/CD8+ T cells in SLE. Lupus Sci Med. 2022; 9(1): e000660. *https://doi.org/10.1136/lupus-2022-000660.*
21. **Schile A, Petrillo M, Vovk A, French R, Leighton K, Dragos Z, et al.** A comprehensive phenotyping program for the MRL-lpr mouse lupus model. J Immunol. 2018; 200:(1_Supplement):40.2. *https://doi.org/10.4049/jimmunol.200.Supp.40.2.*
22. **Zhang D, Wang M, Shi G, Pan P, Ji J, Li P**. Regulating T Cell Population Alleviates SLE by Inhibiting mTORC1/C2 in MRL/lpr Mice. Front Pharmacol. 2021;11: 579298. *https://doi.org/10.3389/fphar.2020.579298.*
23. **Contini P, Negrini S, Murdaca G, Borro M, Puppo F**. Evaluation of membrane-bound and soluble forms of human leucocyte antigen-G in systemic sclerosis. Clin Exp Immunol. 2018;193(2):152-159. *https://doi.org/10.1111/cei.13134.*
24. **Hiramatsu-Asano S, Sunahori-Watanabe K, Zeggar S, Katsuyama E, Mukai T, Morita Y, Wada J.** Deletion of *Mir223* Exacerbates Lupus Nephritis by Targeting *S1pr1* in *Faslpr/lpr* Mice. Front Immunol. 2021;11:616141. *https://doi.org/10.3389/fimmu.2020.616141.*
25. **Barrett JP, Knoblach SM, Bhattacharya S, Gordish-Dressman H, Stoica BA, Loane DJ**. Traumatic Brain Injury Induces cGAS Activation and Type I Interferon Signaling in Aged Mice. Front Immunol. 2021;12:710608. *https://doi.org/10.3389/fimmu.2021.710608.*
26. **Chuang HC, Chen MH, Chen YM, Yang HY, Ciou YR, Hsueh CH, et al.** BPI overexpression suppresses Treg differentiation and induces exosome-mediated inflammation in

systemic lupus erythematosus. Theranostics. 2021;11(20):9953-9966. *https://doi.org/10.7150/thno.63743.*

27. **Sun JK, Zhang WH, Chen WX, Wang X, Mu XW**. Effects of early enteral nutrition on Th17/Treg cells and IL-23/IL-17 in septic patients. World J Gastroenterol. 2019;25(22):2799-2808. *https://doi.org/10.3748/wjg.v25.i22.2799.*
28. **Lourenço JD, Teodoro WR, Barbeiro DF, Velosa APP, Silva LEF, Kohler JB, et al.** Th17/Treg-Related Intracellular Signaling in Patients with Chronic Obstructive Pulmonary Disease: Comparison between Local and Systemic Responses. Cells. 2021;10(7):1569. *https://doi.org/10.3390/cells10071569.*
29. **Li J, Zhao J, Chai Y, Li W, Liu X, Chen Y.** *Astragalus* polysaccharide protects sepsis model rats after cecum ligation and puncture. Front Bioeng Biotechnol. 2022;10:1020300. *https://doi.org/10.3389/fbioe.2022.1020300.*